Paper 250

©Civil-Comp Press, 2012
Proceedings of the Eleventh International Conference
on Computational Structures Technology,
B.H.V. Topping, (Editor),
Civil-Comp Press, Stirlingshire, Scotland

Hierarchical Numerical Modelling of Nested Poroelastic Media

E. Rohan[1] and R. Cimrman[2]
[1]Department of Mechanics, Faculty of Applied Sciences
[2]New Technologies Research Centre
University of West Bohemia, Plzeň, Czech Republic

Abstract

This paper contributes to modelling of porous materials with different levels of porosity at different length scales. We use the theory of homogenization to upscale a poroelastic description of the lowest level to higher levels of porosities in a sense that effective poroelastic material coefficients (consistent with the Biot model) at a higher level are obtained by applying homogenization to the lower level. In this way, different porosities associated with different scale levels are taken into account and a hierarchical description of a macroscopic specimen is obtained. We consider two scales and focus on two important cases: a) the systems of pores at the two scales are interconnected or b) are mutually separated by a semipermeable interface. Homogenization results as well as numerical examples are presented.

Keywords: poroelasticity, homogenization, double porosity, micromechanics, multiscale modelling.

1 Introduction

In nature as well as in technical practice one can often find materials with different levels of porosity at different scales. One possible approach to modelling such materials is to use the theory of porous media combined with the homogenization. A model of poroelasticity [5] can describe behaviour at the mesoscopic scale. To take into account heterogeneities, the theory of homogenization [4, 20] provides a natural way of upscaling from this mesoscopic level to the macroscopic one, whereby effective poroelastic material coefficients (consistent with the Biot model) at a higher level are obtained. This approach leads to a suitable hierarchical description of the porous medium, where different porosities associated with different scale levels are respected. Alternatively the dual porosity ansatz [1, 9, 17] related to strong heterogeneities in the material permeability can be employed, so that one-level homogenization provides a model associated with multiple hierarchies of pores. Besides frequently studied models of fractured porous rocks and other similar materials used in geosciences, an example of a natural hierarchical porosity is the bone tissue, cf. [6]; two porosities, the Haversian and the canaliculo-lacunar, associated with the meso- and micro-scopic levels, respectively, form a connected double-porous structure where deformations induce fluid redistribution.

In the present study we provide homogenization-based formulae which enable to compute the poroelasticity coefficients for a given geometry and topology of micro- and mesoscopic levels. At the microscopic level we consider solid skeleton filled with a compressible fluid. Homogenization at each scale level proceeds in two steps: 1) Find effective (homogenized) coefficients by solving auxiliary problems for several characteristic (or corrector) functions, cf. [17, 13]; 2) Compute the homogenized coefficients that can be used for the higher level and/or "global" (homogenized) model of the current level. Due to linearity of the problems, those steps are decoupled in a sense that the computation of the homogenized coefficients for the global level is valid for any point having the corresponding "microstructure".

We present the two-level upscaling "micro-meso-macro" and illustrate influence of the pore geometry and topology. In [16] we considered systems of interconnected pores at different scales; in a steady state there is only one pore fluid pressure. In this paper, we describe a different arrangement of porosities which can be mutually separated by a semipermeable interface, however, each porosity can form a separate connected system. In this situation, the homogenized problem results in two different pressures. At the mesoscopic scale we take into account the Darcy flow in the poroelastic matrix, although in the mesoscopic fractures (called channels in our terminology) the fluid is assumed to be static with no pressure gradients.

Here we report the main results only, as the derivation of the homogenization formulae is beyond the scope of this paper. In Section 2 we discuss modelling assumptions and introduce all formulae and equations constituting the two-level homogenized model. The hierarchical homogenization is implemented in our in-house finite element code; in Section 3 we illustrate the hierarchical upscaling procedure on two examples.

2 Hierarchical model of double porosity

We consider a poroelastic medium saturated by fluid. The porosity of the medium is formed at two levels, distinguishable by different sizes of pores. These are connected by a weakly permeable interface, so that the model also describes a situation of disconnected porosities.

The two levels, further labeled by superscripts α and β are associated with the "microscale" and the "mesoscale", respectively. At the microscale level, we consider an elastic solid phase forming a porous skeleton filled with fluid. We assume only moderate pressure gradients at the mesoscopic scale, such that no flow dynamic effects are considered at the microscopic scale – the fluid is static. The pores can form a connected porosity, or mutually separated inclusions: in the first case only one scalar pressure value represents the pressure field in the porosity. By homogenizing this two-phase medium we obtain a Biot-type model describing at the mesoscale the upscaled poroelastic microstructure α, cf. [2].

At the mesoscale the above mentioned α-poroelasticity model describes the material occupying the matrix of the meso-structure β; at this "higher" level the canals can exchange the fluid with the microscopic pores of the α level due to a weakly permeable interface. For upscaling from the meso- to the macroscopic scale, we take into account a slow flow in the "dual porosity" associated with the microscopic scale.

Let us consider the scale parameter ε, describing the ratio of the characteristic sizes, L^α and L^β, of the two levels, i.e. $\varepsilon = L^\alpha/L^\beta$. By superscript $^\varepsilon$ we indicate dependence of functions and other parameters on ε. The two-level structure (double porosity) is studied for $\varepsilon \rightarrow 0$ using the periodic unfolding method of homogenization (other methods can be used); first we homogenize the microstructure, thus the effective poroelastic properties of the "matrix" at the level β are obtained. Then upscaling of the level β using analogical procedure with $\varepsilon = L^\beta/L^{\rm macro}$ leads to the effective poroelastic properties of the "macroscopic" level.

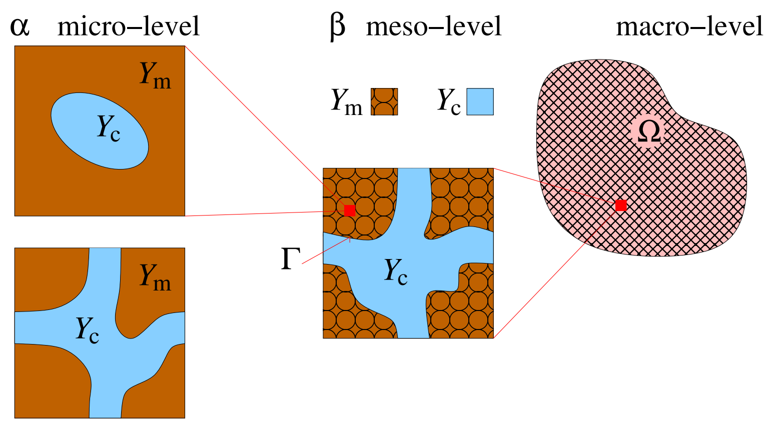

Figure 1: The two-level heterogeneous structure: α-level can be formed by an occluded (disconnected) porosities Y_c^α, or by a single connected porosity; the matrix Y_m^α is formed by the solid. At the β-level, the homogenized structure of the α-level forms the material situated in the matrix Y_m^β. Representative periodic cells are depicted.

2.1 1st level upscaling: micro-to-meso

At the mesoscopic scale we consider domain $\Omega^\alpha \subset \mathbb{R}^3$ which is decomposed into the skeleton and the canals (or inclusions) occupying the domains $\Omega_m^{\alpha,\varepsilon}$ and $\Omega_c^{\alpha,\varepsilon}$, which are separated by the interface $\Gamma^{\alpha,\varepsilon}$,

$$\Omega^\alpha = \Omega_m^{\alpha,\varepsilon} \cup \Omega_c^{\alpha,\varepsilon} \cup \Gamma^{\alpha,\varepsilon}\,, \quad \Omega_m^{\alpha,\varepsilon} \cap \Omega_c^{\alpha,\varepsilon} = \emptyset\,, \qquad \Gamma^{\alpha,\varepsilon} = \overline{\Omega_m^{\alpha,\varepsilon}} \cap \overline{\Omega_c^{\alpha,\varepsilon}}\,. \quad (1)$$

In what follows, we will denote by ∇ and $\nabla\cdot$ the gradient and divergence operators, respectively. The symbol "$\cdot$" will denote the scalar product and the symbol ":" between tensors of any orders denotes their double contraction. $\boldsymbol{e}(\boldsymbol{u})$ is the linear strain tensor generated by displacement vector $\boldsymbol{u}$.

2.1.1 Model at the microscopic scale

The deformation of the matrix is governed by the system of equations defining the α-level problem: find $(\boldsymbol{u}^{\alpha,\varepsilon}, p^{\alpha,\varepsilon})$ such that

$$
\begin{aligned}
\nabla \cdot (\mathbb{D}^{\alpha,\varepsilon}\boldsymbol{e}(\boldsymbol{u}^{\alpha,\varepsilon})) &= \boldsymbol{f}^{\alpha,\varepsilon} \;, \quad \text{in } \Omega_m^{\alpha,\varepsilon} \;,\\
\boldsymbol{n}^{[m]} \cdot \mathbb{D}^{\alpha,\varepsilon}\boldsymbol{e}(\boldsymbol{u}^{\alpha,\varepsilon}) &= \boldsymbol{g}^{\alpha,\varepsilon} \;, \quad \text{on } \partial_{\text{ext}}\Omega_m^{\alpha,\varepsilon} \;,\\
\boldsymbol{n}^{[m]} \cdot \mathbb{D}^{\alpha,\varepsilon}\boldsymbol{e}(\boldsymbol{u}^{\alpha,\varepsilon}) &= -p^{\alpha,\varepsilon}\boldsymbol{n}^{[m]} \;, \quad \text{on } \Gamma^{\alpha,\varepsilon} \;,
\end{aligned}
\tag{2}
$$

and

$$
\int_{\partial\Omega_c^{\alpha,\varepsilon}} \boldsymbol{u}^{\alpha,\varepsilon} \cdot \boldsymbol{n}^{[c]} \, \mathrm{dS}_x + \gamma^\alpha p^{\alpha,\varepsilon} |\Omega_c^{\alpha,\varepsilon}| = -J^{\alpha,\varepsilon} \;, \tag{3}
$$

where $\boldsymbol{u}^{\alpha,\varepsilon}$ is the displacement vector of the matrix, $p^{\alpha,\varepsilon}$ is the fluid pressure, $\mathbb{D}^{\alpha,\varepsilon}$ is the fourth-order elasticity tensor of the matrix and γ^α is the fluid compressibility. The applied surface-force and volume-force fields are denoted respectively by $\boldsymbol{g}^{\alpha,\varepsilon}$ and $\boldsymbol{f}^{\alpha,\varepsilon}$. The outer unit normal vector of the boundary $\Omega_m^{\alpha,\varepsilon}$ is denoted by $\boldsymbol{n}^{[m]}$. Condition (3) says that the change of the porosity (the first left-hand side term), i.e., change of volume $|\Omega_c^{\alpha,\varepsilon}|$, is compensated by fluid compression and by the fluid out-flow $J^{\varepsilon,\alpha}$ through external boundary $\partial_{\text{ext}}\Omega_c^{\alpha,\varepsilon} = \partial\Omega_c^{\alpha,\varepsilon} \cup \partial\Omega^\alpha$, *i.e.* outwards Ω^α. Note that the solvability condition yields $\int_{\partial_{\text{ext}}\Omega_m^{\alpha,\varepsilon}} \boldsymbol{g}^{\alpha,\varepsilon} \, \mathrm{dS}_x + \int_{\Omega_m^{\alpha,\varepsilon}} \boldsymbol{f}^{\alpha,\varepsilon} \, \mathrm{dV}_x = \mathbf{0}$ where dS_x and dV_x are the differential elements of surface and volume, respectively.

The boundary value problem given by (2) and (3) can be reformulated in the weak sense: find $(\boldsymbol{u}^{\alpha,\varepsilon}, p^{\alpha,\varepsilon}) \in \mathbf{H}^1(\Omega_m^{\alpha,\varepsilon})/\boldsymbol{\mathcal{R}}(\Omega^\alpha) \times \mathbb{R}$ such that

$$
\begin{aligned}
&\int_{\Omega_m^{\alpha,\varepsilon}} (\mathbb{D}^{\alpha,\varepsilon}\boldsymbol{e}(\boldsymbol{u}^{\alpha,\varepsilon})) : \boldsymbol{e}(\boldsymbol{v}) \, \mathrm{dV}_x + p^{\alpha,\varepsilon} \int_{\Gamma_m^{\alpha,\varepsilon}} \boldsymbol{n}^{[m]} \cdot \boldsymbol{v} \, \mathrm{dS}_x = \\
&\qquad \int_{\partial_{\text{ext}}\Omega_m^{\alpha,\varepsilon}} \boldsymbol{g}^{\alpha,\varepsilon} \cdot \boldsymbol{v} \, \mathrm{dS}_x + \int_{\Omega_m^{\alpha,\varepsilon}} \boldsymbol{f}^{\alpha,\varepsilon} \cdot \boldsymbol{v} \, \mathrm{dV}_x, \qquad \text{for all } \boldsymbol{v} \in \mathbf{H}^1(\Omega_m^{\alpha,\varepsilon}) \;,
\end{aligned}
\tag{4}
$$

$$
\int_{\partial\Omega_c^{\alpha,\varepsilon}} \boldsymbol{u}^{\alpha,\varepsilon} \cdot \boldsymbol{n}^{[c]} \, \mathrm{dS}_x + \gamma^\alpha p^{\alpha,\varepsilon} |\Omega_c^{\alpha,\varepsilon}| = -J^{\alpha,\varepsilon} \;,
$$

where space $\boldsymbol{\mathcal{R}}(\Omega^\alpha)$ contains all the rigid body motions; due to the boundary conditions in (2), the displacements are determined up to rigid body motions. We assume that $\boldsymbol{f}^{\alpha,\varepsilon}$ and $\boldsymbol{g}^{\alpha,\varepsilon}$ are defined in such a way that the solvability conditions associated with (4) are satisfied.

2.1.2 Homogenization result

We assume that the domain Ω^α is obtained from a periodic microstructure generated by a representative unit cell Y^α decomposed as follows

$$Y^\alpha = Y_m^\alpha \cup Y_c^\alpha \cup \Gamma_Y^\alpha \;, \quad Y_c^\alpha = Y^\alpha \setminus Y_m^\alpha \;, \quad \Gamma_Y^\alpha = \overline{Y_m^\alpha} \cap \overline{Y_c^\alpha} \;. \tag{5}$$

Without loss of generality we can define $Y = (]0,1[)^3$ to be the unit cube, so $|Y| = 1$. As a result of (5), the domain Ω^α is defined by $\bigcup_{k\in\mathbb{K}^\varepsilon} \varepsilon(Y^\alpha + k)$ with $\mathbb{K}^\varepsilon = \{k \in \mathbb{Z}^3, \varepsilon(Y^\alpha + k) \subset \Omega^\alpha\}$. The upscaling procedure of the heterogeneous continuum consists in the limit analysis with respect to $\varepsilon \to 0$. For this we use the periodic unfolding method [4, 8] based on the coordinate decomposition $x = \xi + \varepsilon y$, where $\xi = \varepsilon \left[\frac{x}{\varepsilon}\right]_Y$ is the lattice coordinate at the mesoscopic scale, so that $y \in Y$ is the local coordinate of the microscopic scale. The analogous notation is employed when upscaling from the mesoscopic to macroscopic scale. By $⨍_D = |Y|^{-1} \int_D$ with $D \subset \overline{Y}$ we denote the local average, although $|Y| = 1$.

We assume weak convergence of the external forces; denoting by χ_m^ε the characteristic function of the matrix, $\chi_m^\varepsilon \boldsymbol{f}^{\alpha,\varepsilon}$ converge towards $(1-\phi^\alpha)\boldsymbol{f}^\alpha$ where $\boldsymbol{f}^\alpha$ is a local averaged volume-force acting on the matrix. The volume fraction of pores is defined by $\phi^\alpha = |Y_c^\alpha|/|Y^\alpha|$.

When $\varepsilon \to 0$, the strain is a two-scale function defined from its macroscopic part $\boldsymbol{e}(\boldsymbol{u}(x))$ and its fluctuating part $\boldsymbol{e}_y(\boldsymbol{u}^1(x,y))$, where the fluctuations are proportional to macroscopic strains. There are so called characteristic displacements $\boldsymbol{\omega}^{ij}(y)$ and $\boldsymbol{\omega}^P(y)$ such that $\boldsymbol{u}^1(x,y) = \boldsymbol{\omega}^{ij}(y)\partial_j u_i(x) - \boldsymbol{\omega}^P(y)p$, where p is the constant fluid pressure in Ω^α. Functions $\boldsymbol{\omega}^{ij}(y)$ and $\boldsymbol{\omega}^P(y)$ are obtained as solutions of the following problems: find $(\boldsymbol{\omega}^{ij}, \boldsymbol{\omega}^P) \in \mathbf{H}^1_\#(Y_m) \times \mathbf{H}^1_\#(Y_m)$ satisfying

$$\begin{aligned} a_m^\alpha\left(\boldsymbol{\omega}^{ij} + \boldsymbol{\Pi}^{ij},\, \boldsymbol{v}\right) &= 0 \;, \quad \forall \boldsymbol{v} \in \mathbf{H}^1_\#(Y_m) \;, \\ a_m^\alpha\left(\boldsymbol{\omega}^P,\, \boldsymbol{v}\right) &= ⨍_{\Gamma_Y} \boldsymbol{v} \cdot \boldsymbol{n}^{[m]} \,\mathrm{dS}_y \;, \quad \forall \boldsymbol{v} \in \mathbf{H}^1_\#(Y_m) \;, \end{aligned} \tag{6}$$

where $a_m^\alpha(\boldsymbol{w},\, \boldsymbol{v}) = ⨍_{Y_m} (\mathbb{D}\boldsymbol{e}_y(\boldsymbol{w})) : \boldsymbol{e}_y(\boldsymbol{v})$ and $\boldsymbol{\Pi}^{ij} = (\Pi_k^{ij})$, $i,j,k = 1,2,3$ with $\Pi_k^{ij} = y_j \delta_{ik}$.

Using the characteristic responses (6) obtained at the microscopic scale the effective properties of the deformable porous medium are given by

$$A_{ijkl}^\alpha = a_m^\alpha\left(\boldsymbol{\omega}^{ij} + \boldsymbol{\Pi}^{ij},\, \boldsymbol{\omega}^{kl} + \boldsymbol{\Pi}^{kl}\right) \;, \quad B_{ij}^\alpha = -⨍_{Y_m} \mathrm{div}_y \boldsymbol{\omega}^{ij} \;, \quad M^\alpha = a_m^\alpha\left(\boldsymbol{\omega}^P,\, \boldsymbol{\omega}^P\right) \;. \tag{7}$$

Obviously, the tensors $\mathbb{A}^\alpha = (A_{ijkl}^\alpha)$ and $\boldsymbol{B}^\alpha = (B_{ij}^\alpha)$ are symmetric; moreover $\mathbb{A}^\alpha$ is positive definite and $M^\alpha > 0$.

Model of the poroelasticity At this first-level of the homogenization process, we obtain a model of the poroelasticity involving the skeleton displacements $\boldsymbol{u} \in \mathbf{H}^1(\Omega)/\boldsymbol{\mathcal{R}}(\Omega)$

and fluid pressure $p \in \mathbb{R}$ which is constant due to our assumptions. These state variables verify the following equations:

$$
\begin{aligned}
&\int_\Omega \left(\mathbb{A}^\alpha \boldsymbol{e}(\boldsymbol{u}) - p\hat{\boldsymbol{B}}^\alpha\right) : \boldsymbol{e}(\boldsymbol{v}) = \int_\Omega (1-\phi)\boldsymbol{f}\cdot\boldsymbol{v} + \int_{\partial\Omega} \bar{\boldsymbol{g}}\cdot\boldsymbol{v}\,\mathrm{dS}_x\;, \quad \forall \boldsymbol{v} \in \mathbf{H}^1(\Omega)\;,\\
&\int_\Omega \hat{\boldsymbol{B}}^\alpha : \boldsymbol{e}(\boldsymbol{u}) + p(M^\alpha + \phi^\alpha\gamma)|\Omega^\alpha| = -J, \quad \text{with } \hat{\boldsymbol{B}}^\alpha := \boldsymbol{B}^\alpha + \phi^\alpha \mathbf{I},
\end{aligned}
\tag{8}
$$

where J is the limit of the total flux $J^{\alpha,\varepsilon}$ outwards Ω^α and $\bar{\boldsymbol{g}}$ is the mean surface stress (traction force).

2.2 2nd level upscaling: meso-to-macro

The dimensionless parameter ε now denotes the ratio between the mesoscopic and the macroscopic scales. At the mesoscopic scale, the geometrical configuration consists of two compartments: 1) the *matrix* $\Omega_m^{\beta,\varepsilon}$ which is formed by the porous medium associated with the upscaled microstructure of level α, 2) the *channels* $\Omega_c^{\beta,\varepsilon}$ which are filled with the fluid. The following split holds: $\Omega^\beta = \Omega_m^{\beta,\varepsilon} \cup \Omega_c^{\beta,\varepsilon} \cup \Gamma^{\beta,\varepsilon}$. The interface $\Gamma_m^{\beta,\varepsilon}$ separating the two compartments is semipermeable, in general, i.e. the fluid can be redistributed between $\Omega_m^{\beta,\varepsilon}$ and $\Omega_c^{\beta,\varepsilon}$. As well as in the case of the 1st level upscaling, we neglect any pressure gradients in the fluid occupying $\Omega_c^{\beta,\varepsilon}$.

2.2.1 Model at the mesoscopic scale

The structure is loaded on $\partial_{\text{ext}}\Omega_m^{\beta,\varepsilon} = \partial\Omega^\beta \cap \partial\Omega_m^{\beta,\varepsilon}$ by a surface-force field $\bar{\boldsymbol{g}}^\alpha$ (see (8)) and by a volume-force field $\hat{\boldsymbol{f}}^\alpha = (1-\phi^\alpha)\boldsymbol{f}$ acting on the solid phase. The total outflow from Ω^β through the micro-porosity α is $J_{\text{ext}}^{\beta,\varepsilon}$. Moreover, the mesoscopic channels of the level β are drained through $\partial_{\text{ext}}\Omega_c^{\beta,\varepsilon}$; we assume that a normal filtration velocity $\bar{w}_n$ is given.

Pressure at the mesoscopic level By $\tilde{p}^{\alpha,\varepsilon}$ we shall refer to the pressure in the upscaled "microscopic" porosity, i.e. in $\Omega_m^{\beta,\varepsilon}$, whereas by $p^{\beta,\varepsilon}$ we denote the fluid pressure in the mesoscopic pores which form $\Omega_c^{\beta,\varepsilon}$. Further, $p^\varepsilon = (\tilde{p}^{\alpha,\varepsilon}, p^{\beta,\varepsilon})$ is the abbreviation for pressure in Ω^β.

Using the result of the upscaling of the α-level problem, the poroelasticity model (8) yields the following equilibrium equations imposed locally in any $x \in \Omega_m^{\beta,\varepsilon}$

$$
\begin{aligned}
-\nabla\cdot\boldsymbol{\sigma}^{\beta,\varepsilon} &= (1-\phi^\alpha)\boldsymbol{f}\;,\\
\phi^\alpha\dot{\zeta}^{\beta,\varepsilon} + \hat{\boldsymbol{B}}^\alpha : \boldsymbol{e}(\dot{\boldsymbol{u}}^{\beta,\varepsilon}) + (M^\alpha + \phi^\alpha\gamma)\dot{\tilde{p}}^{\alpha,\varepsilon} &= 0\;,
\end{aligned}
\tag{9}
$$

where $\dot{\zeta}^{\beta,\varepsilon}$ is the local increase of the fluid volume in the 1st level porosity. Moderate pressure gradients $\nabla\tilde{p}^{\alpha,\varepsilon}$ are admitted at the mesoscale level in $\Omega_m^{\beta,\varepsilon}$, so that (9) is supplemented by the constitutive equations involving a permeability tensor $\boldsymbol{K}$:

$$
\begin{aligned}
\boldsymbol{\sigma}^{\beta,\varepsilon} &= \mathbb{A}^\alpha\boldsymbol{e}(\boldsymbol{u}^{\beta,\varepsilon}) - \hat{\boldsymbol{B}}^\alpha\tilde{p}^{\alpha,\varepsilon}\;,\\
\phi^\alpha\dot{\zeta}^{\beta,\varepsilon} &= -\nabla\cdot\boldsymbol{w}^{\beta,\varepsilon}\;, \quad \boldsymbol{w}^{\beta,\varepsilon} = -\boldsymbol{K}\nabla\tilde{p}^{\alpha,\varepsilon}\;.
\end{aligned}
\tag{10}
$$

While the stress $\boldsymbol{\sigma}$ is given according to $(8)_1$, $\boldsymbol{w}^{\beta,\varepsilon}$ is the filtration velocity obeying the Darcy law. The permeability $\boldsymbol{K}$ can be computed using the standard homogenization of the Stokes flow considered in a connected α-porosity generated by Y_c^α, see e.g. [9, 20]. However, if this porosity is not connected, i.e. if $\overline{Y_c^\alpha} \cap \partial Y = \emptyset$, then $\boldsymbol{K}$ is zero! In this case also the interface Γ_m^β is impermeable.

On the interface $\Gamma_m^{\beta,\varepsilon}$ separating the pore fluid and the poroelastic matrix the following conditions are considered,

$$
\begin{aligned}
\boldsymbol{n} \cdot \boldsymbol{\sigma}^{\beta,\varepsilon} &= \boldsymbol{n} p^{\beta,\varepsilon} \;, \\
-\boldsymbol{n} \cdot \boldsymbol{K} \nabla \tilde{p}^{\alpha,\varepsilon} &= \varkappa^\varepsilon [p^\varepsilon]_\beta^\alpha \;, \qquad \text{where } [p^\varepsilon]_\beta^\alpha = (\tilde{p}^{\alpha,\varepsilon} - p^{\beta,\varepsilon}) \;,
\end{aligned}
\tag{11}
$$

which express pressure loading of the solid phase of the microscopic porosity, $(11)_1$, and the semipermeability of $\Gamma_m^{\beta,\varepsilon}$, $(11)_2$. We shall assume

$$
\varkappa^\varepsilon = \varepsilon \bar{\varkappa} \;,
$$

so that the interface is progressively less permeable with decreasing size of the mesoscopic structure. Note that $\bar{\varkappa} = 0$ if the α porosity is occluded, as discussed above.

It is now possible to set the β-level problem: find $(\boldsymbol{u}^{\beta,\varepsilon}, \tilde{p}^{\alpha,\varepsilon}, p^{\beta,\varepsilon}) \in \mathbf{H}^1(\Omega_m^{\beta,\varepsilon}) \times H^1(\Omega_m^{\beta,\varepsilon}) \times \mathbb{R}$ such that

$$
\begin{aligned}
&\int_{\Omega_m^{\beta,\varepsilon}} \left(\mathbb{A}^\alpha : \boldsymbol{e}(\boldsymbol{u}^{\beta,\varepsilon}) - \tilde{p}^{\alpha,\varepsilon} \hat{\boldsymbol{B}}^\alpha \right) : \boldsymbol{e}(\boldsymbol{v}) + p^{\beta,\varepsilon} \int_{\Gamma^{\beta,\varepsilon}} \boldsymbol{v} \cdot \boldsymbol{n}^{[m]} \, \mathrm{dS}_x = \\
&\qquad\qquad \int_{\Omega_m^{\beta,\varepsilon}} \hat{\boldsymbol{f}}^\alpha \cdot \boldsymbol{v} + \int_{\partial_{\mathrm{ext}} \Omega_m^{\beta,\varepsilon}} \bar{\boldsymbol{g}}^\alpha \, \mathrm{dS}_x \;, \\
&\int_{\Omega_m^{\beta,\varepsilon}} \left(\hat{\boldsymbol{B}}^\alpha : \boldsymbol{e}(\dot{\boldsymbol{u}}^{\beta,\varepsilon}) + (M^\alpha + \gamma \phi^\alpha) \dot{\tilde{p}}^{\alpha,\varepsilon} \right) q^\alpha + \int_{\Omega_m^{\beta,\varepsilon}} \boldsymbol{K} \nabla \tilde{p}^{\alpha,\varepsilon} \cdot \nabla q^{\alpha,\varepsilon} \\
&\quad + \int_{\Gamma^{\beta,\varepsilon}} \varkappa^\varepsilon [p^\varepsilon]_\beta^\alpha [q^\varepsilon]_\beta^\alpha + q^\beta \int_{\Gamma^{\beta,\varepsilon}} \dot{\boldsymbol{u}}^{\beta,\varepsilon} \cdot \boldsymbol{n}^{[c]} \, \mathrm{dS}_x + \gamma \phi^\beta |\Omega^\beta| \dot{p}^{\beta,\varepsilon} q^\beta = \\
&\qquad\qquad -J_{\mathrm{ext}}^\beta q^\beta + \int_{\partial_{\mathrm{ext}} \Omega_m^{\beta,\varepsilon}} q^\alpha \boldsymbol{n}^{[m]} \cdot \bar{\boldsymbol{w}}^\varepsilon \;,
\end{aligned}
\tag{12}
$$

for all $\boldsymbol{v} \in \mathbf{H}^1(\Omega_m^{\beta,\varepsilon})$ and for all $q^\alpha \in H^1(\Omega_m^{\beta,\varepsilon})$. Problem (12) has been treated by asymptotic analysis, $\varepsilon \to 0$. Below we summarize the main results. We recall $1 - \phi^{\beta,\varepsilon} = |\Omega_m^{\beta,\varepsilon}| / |\Omega^\beta|$, where $\phi^{\beta,\varepsilon} \to \phi^\beta := |Y_c^\beta| / |Y^\beta|$.

2.2.2 Homogenization result

In analogy with the first level upscaling, we consider a periodic mesostructure generated by the local periodic cell Y^β which is decomposed according to (5), i.e. $Y^\beta = Y_m^\beta \cup Y_c^\beta \cup \Gamma_Y^\beta$. To define the local problems for corrector functions, we need the following bilinear forms which involve the homogenized coefficients computed in (7):

$$
\begin{aligned}
a_m^\beta(\boldsymbol{w}, \boldsymbol{v}) &= \fint_{Y_m^\beta} \mathbb{A}^\alpha \boldsymbol{e}_y(\boldsymbol{w}) : \boldsymbol{e}_y(\boldsymbol{v}) \;, \\
b_m^\beta(p, \boldsymbol{v}) &= \fint_{Y_m^\beta} p \hat{\boldsymbol{B}}^\alpha : \boldsymbol{e}_y(\boldsymbol{v}) \;.
\end{aligned}
\tag{13}
$$

Obviously, $a_m^\beta(\cdot,\,\cdot)$ is coercive on $\mathbf{H}^1_\#(Y_m^\beta)$. The convergence result yields multiplicative splits of the displacement and pressure fluctuations, $\boldsymbol{u}^1$ and p^1:

$$
\begin{aligned}
&\boldsymbol{u}^1(x,y,t) = \boldsymbol{w}^{ij} e^x_{ij}(\boldsymbol{u}) + \hat{\boldsymbol{w}}(y) p^\alpha(x,t) + \bar{\boldsymbol{w}}(y)\bar{p}^\beta(t)\;,\\
&p^1(x,y,t) = \eta^i \partial_i^x p^\alpha(x,t)\;.
\end{aligned}
$$

It is worth noting that upscaling from the meso- to the macro-level does not lead to any fading memory terms involving time convolutions, in contrast with upscaling of the double porosity media, cf. [17, 12]. As a counterpart to the α level, see (6), the characteristic responses, i.e., displacement modes at the mesoscopic level, satisfy the following problems: find $\boldsymbol{w}^{ij}, \hat{\boldsymbol{w}}, \bar{\boldsymbol{w}} \in \mathbf{H}^1_\#(Y_m^\beta)$ such that

$$
\begin{aligned}
a_m^\beta\left(\boldsymbol{w}^{ij} + \boldsymbol{\Pi}^{ij},\, \boldsymbol{v}\right) = 0 \quad \forall \boldsymbol{v} \in \mathbf{H}^1_\#(Y_m^\beta)\;,&\\
a_m^\beta\left(\hat{\boldsymbol{w}},\, \boldsymbol{v}\right) = b_m^\beta\left(1,\, \boldsymbol{v}\right) \quad \forall \boldsymbol{v} \in \mathbf{H}^1_\#(Y_m^\beta)\;,&\\
a_m^\beta\left(\bar{\boldsymbol{w}},\, \boldsymbol{v}\right) = -\int\!\!\!\!\!\!-_{\Gamma_Y^\beta} \boldsymbol{v}\cdot\boldsymbol{n}^{[m]} \quad \forall \boldsymbol{v} \in \mathbf{H}^1_\#(Y_m^\beta)\;.&
\end{aligned}
\tag{14}
$$

The pressure fluctuation p^1 associated with the α-level porosity is driven by the characteristic pressure response: find $\eta^1 \in H^1_\#(Y_m^\beta)/\mathbb{R}$ such that

$$
\int\!\!\!\!\!\!-_{Y_m^\beta} \boldsymbol{K}\nabla_y(\eta^i + y_i)\cdot\nabla_y\psi = 0 \quad \forall \boldsymbol{v} \in H^1_\#(Y_m^\beta)\;. \tag{15}
$$

The homogenized coefficients describing the material behaviour at the β level are computed as follows:

$$
\begin{aligned}
\mathbb{A}^\beta = (A^\beta_{ijkl}),\quad & A^\beta_{ijkl} = a_m^\beta\left(\boldsymbol{w}^{ij} + \boldsymbol{\Pi}^{ij},\, \boldsymbol{w}^{kl} + \boldsymbol{\Pi}^{kl}\right)\;,\\
\boldsymbol{B}^\beta = (B^\beta_{ij}),\quad & B^\beta_{ij} = b_m^\beta\left(1,\, \boldsymbol{w}^{ij} + \boldsymbol{\Pi}^{ij}\right)\;,\\
\bar{\boldsymbol{B}}^\beta = (\bar{B}^\beta_{ij}),\quad & \bar{B}^\beta_{ij} = \phi^\beta\delta_{ij} + a_m^\beta\left(\boldsymbol{w}^{ij},\, \bar{\boldsymbol{w}}\right)\;,\\
\boldsymbol{K}^\beta = (K^\beta_{ij}),\quad & K^\beta_{ij} = \int\!\!\!\!\!\!-_{Y_m^\beta} \boldsymbol{K}\nabla_y(\eta^i + y_i)\cdot\nabla_y(\eta^j + y_j)\;,
\end{aligned}
\tag{16}
$$

where $\mathbb{A}^\beta$ is the skeleton stiffness corresponding to the dried medium, $\boldsymbol{B}^\beta$ and $\bar{\boldsymbol{B}}^\beta$ are the Biot-type stress coefficients associated with the two pressures, p^α and $\bar{p}^\beta$, respectively, and $\boldsymbol{K}^\beta$ is the effective permeability.

There are three effective Biot compressibility modulae

$$
M^\beta = a_m^\beta\left(\hat{\boldsymbol{w}},\, \hat{\boldsymbol{w}}\right)\;,\quad \bar{M}^\beta = a_m^\beta\left(\bar{\boldsymbol{w}},\, \bar{\boldsymbol{w}}\right)\;,\quad N^\beta = a_m^\beta\left(\hat{\boldsymbol{w}},\, \bar{\boldsymbol{w}}\right)\;, \tag{17}
$$

which constitute the following compressibility matrix:

$$
\mathbb{M}^\beta = \begin{bmatrix} M^\beta + M^\alpha + \gamma\phi^\alpha & N^\beta \\ N^\beta & \bar{M}^\beta + \gamma\phi^\beta \end{bmatrix}\;. \tag{18}
$$

Further, we shall use the two-level pressure $[p^\alpha, \bar{p}^\beta] \in L^2(\Omega^\beta)\times\mathbb{R}$, recalling that $\bar{p}^\beta$ is a scalar value. The macroscopic behaviour of the double porosity fluid saturated medium is described by the triplet $(\boldsymbol{u}, p^\alpha, \bar{p}^\beta) \in \mathbf{H}^1(\Omega^\beta)/\mathcal{R}(\Omega^\beta) \times L^2(\Omega^\beta) \times \mathbb{R}$ which satisfies the macroscopic equations (we use the abbreviation $\Omega = \Omega^\beta$)

$$\int_\Omega \mathbb{A}^\beta \boldsymbol{e}(\boldsymbol{u}) : \boldsymbol{e}(\boldsymbol{v}) - \int_\Omega \boldsymbol{e}(\boldsymbol{v}) : \left[\boldsymbol{B}^\beta, \bar{\boldsymbol{B}}^\beta\right] [p^\alpha, \bar{p}^\beta]^T = \int_{\partial\Omega} \bar{\boldsymbol{g}}^\beta \cdot \boldsymbol{v} \, \mathrm{dS}_x + \int_\Omega (1-\phi^\beta) \hat{\boldsymbol{f}}^\alpha \cdot \boldsymbol{v} \; ,$$

$$\begin{aligned} &\int_\Omega [q^\alpha, \bar{q}^\beta] \left[\boldsymbol{B}^\beta, \bar{\boldsymbol{B}}^\beta\right]^T : \boldsymbol{e}(\dot{\boldsymbol{u}}) \\ &+ \int_\Omega \boldsymbol{K}^\beta \nabla p^\alpha \cdot \nabla q^\alpha + \int_\Omega \kappa^\beta (p^\alpha - \bar{p}^\beta)(q^\alpha - \bar{q}^\beta) \\ &\qquad + \int_\Omega [q^\alpha, \bar{q}^\beta] \cdot \mathbf{M}^\beta [\dot{p}^\alpha, \dot{\bar{p}}^\beta]^T = -J^\beta_{\mathrm{ext}} \bar{q}^\beta + \int_{\partial\Omega} (1-\phi^\beta) q^\alpha \bar{w}_n \, \mathrm{dS}_x \; , \end{aligned} \tag{19}$$

for all triplets $(\boldsymbol{v}, q^\alpha, \bar{q}^\beta) \in \mathbf{H}^1(\Omega^\beta) \times L^2(\Omega^\beta) \times \mathbb{R}$, where $\kappa^\beta = \fint_{\Gamma^\beta_Y} \bar{\varkappa}$ is the average interface permeability, $\bar{\boldsymbol{g}}^\beta := (1-\phi^\beta)\bar{\boldsymbol{g}}^\alpha + \phi^\beta(-\bar{p}^\beta)\boldsymbol{n}$ is the mean surface stress (the traction force density), $\bar{w}_n$ is a draining flux outwards the α porosity and J^β_{ext} is a given overall drainage of the β-level connected pores. Obviously, the data must satisfy some solvability conditions.

If $\boldsymbol{K}^\beta$ or κ^β are nonvanishing, initial conditions must be supplied; one may consider the unloaded and undeformed state, or a steady state characterized by a single pressure value, i.e. $p^\alpha(x, \cdot) = \bar{p}^\beta(\cdot)$, $x \in \Omega^\beta$.

3 Numerical examples

The homogenization results presented in previous sections were discretized by the finite element method and implemented in a standalone computer code based on our code SfePy [3]. In this section we show several results obtained by this code.

For numerical illustration of effects of connected versus disconnected porosities on the level α (recall Fig. 1) we used the reference periodic cells of the micro structures shown in Fig. 2. Two cases were considered:

- **case 1**: disconnected porosity on the level α (Fig. 2 left), connected porosity on the level β (Fig. 2 right);

- **case 2**: connected porosity on the levels α and β (Fig. 2 right).

The following material/geometrical parameters were used:

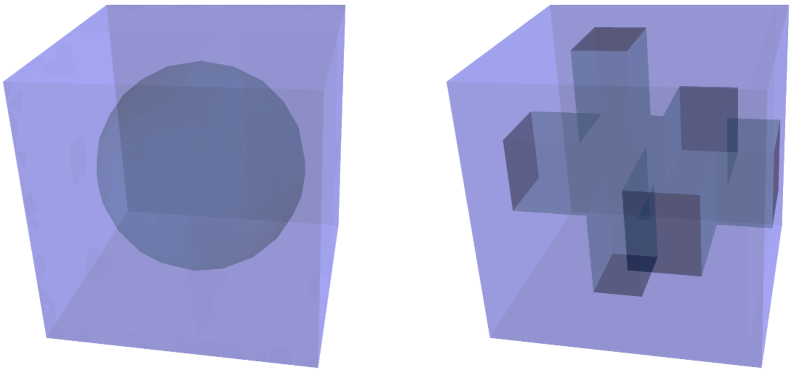

Figure 2: Left: reference cell with disconnected porosity (level α for case 1). Right: reference cell with connected porosity (level α for case 2, level β for cases 1 and 2).

coefficient	units	where	level	values
stiffness $\mathbb{D}$	GPa	Y_m	α	$\lambda = 17$, $\mu = 1.7$
kinematic fluid viscosity ν	m^2/s	Y_c	α	$\nu = 10^{-6}$
fluid compressibility γ	GPa^{-1}	Ω^β	macro β	$\gamma = 1.0$
interface permeability κ^β	m / (GPa s)	Ω^β	macro β	$\kappa^\beta = 10^{-6}$
porosity ϕ	1	case 1	α	$\phi = 0.260$
	1	case 2	α	$\phi = 0.185$
	1	case 1, 2	β	$\phi = 0.185$

where the Lamé parameters defined the stiffness tensor as follows:

$$\mathbb{D} : D_{ijkl} \equiv \mu(\delta_{ik}\delta_{jl} + \delta_{il}\delta_{jk}) + \lambda\delta_{ij}\delta_{kl} \ .$$

Because a practical computation has to be related to a real scale of an existing microstructure, and because of scaling assumptions for fluid viscosity and interface permeability, we assumed the real value of $\varepsilon = 10^{-3}$ and scaled the values given above accordingly, when solving for the homogenized coefficients ($\nu \rightarrow \nu/\varepsilon^2$, $\kappa^\beta \rightarrow \kappa^\beta/\varepsilon$). The computations resulted in the homogenized coefficients summarized in Tab. 1 for the two cases.

The macroscopic equations of level β (19) were solved on a cube domain with the following initial and boundary conditions:

- $\boldsymbol{u}(0,\cdot) = 0$, $p^\alpha(0,\cdot) = 0$, $\bar{p}^\beta(0,\cdot) = 0$,
- $\boldsymbol{u}(t,x) = 0$ for x on the bottom face,
- pressure traction load on the top face, with magnitude equal to time step $\times 10^{-2}$ [GPa] up to step 10, then held on the value 10×10^{-2}, for 20 time steps, $t \in [0, 0.1]$.

In Fig. 3 we compare time histories of macroscopic solutions for the two cases and in Fig. 4 several snapshots of macroscopic solutions are shown. It can be seen that the

coef.	case 1	case 2
$\boldsymbol{K}^\alpha$	$\begin{bmatrix} 0 & 0 & 0 \\ 0 & 0 & 0 \\ 0 & 0 & 0 \end{bmatrix}$	$\begin{bmatrix} 2.05 \cdot 10^{-4} & 0 & 0 \\ 0 & 1.25 \cdot 10^{-4} & 0 \\ 0 & 0 & 2.98 \cdot 10^{-4} \end{bmatrix}$
$\boldsymbol{B}^\alpha$	$[4.70 \cdot 10^{-1}, 4.70 \cdot 10^{-1}, 4.70 \cdot 10^{-1}, 0, 0, 0]$	$[5.87 \cdot 10^{-1}, 5.94 \cdot 10^{-1}, 5.85 \cdot 10^{-1}, 0, 0, 0]$
$\boldsymbol{A}^\alpha$	$\begin{bmatrix} 6.48 & 4.12 & 4.11 & 0 & 0 & 0 \\ 4.12 & 6.50 & 4.12 & 0 & 0 & 0 \\ 4.11 & 4.12 & 6.49 & 0 & 0 & 0 \\ 0 & 0 & 0 & 1.01 & 0 & 0 \\ 0 & 0 & 0 & 0 & 1.01 & 0 \\ 0 & 0 & 0 & 0 & 0 & 1.01 \end{bmatrix}$	$\begin{bmatrix} 5.82 & 3.18 & 3.42 & 0 & 0 & 0 \\ 3.18 & 5.54 & 3.30 & 0 & 0 & 0 \\ 3.42 & 3.30 & 5.84 & 0 & 0 & 0 \\ 0 & 0 & 0 & 0.948 & 0 & 0 \\ 0 & 0 & 0 & 0 & 1.10 & 0 \\ 0 & 0 & 0 & 0 & 0 & 1.05 \end{bmatrix}$
M^α	$2.59 \cdot 10^{-2}$	$3.25 \cdot 10^{-2}$
$\boldsymbol{K}^\beta$	$\begin{bmatrix} 0 & 0 & 0 \\ 0 & 0 & 0 \\ 0 & 0 & 0 \end{bmatrix}$	$\begin{bmatrix} 1.67 \cdot 10^{-4} & 0 & 0 \\ 0 & 1.02 \cdot 10^{-4} & 0 \\ 0 & 0 & 2.43 \cdot 10^{-4} \end{bmatrix}$
$\boldsymbol{B}^\beta$	$[2.84 \cdot 10^{-1}, 2.74 \cdot 10^{-1}, 2.86 \cdot 10^{-1}, 0, 0, 0]$	$[3.31 \cdot 10^{-1}, 3.30 \cdot 10^{-1}, 3.28 \cdot 10^{-1}, 0, 0, 0]$
$\bar{\boldsymbol{B}}^\beta$	$[3.15 \cdot 10^{-1}, 3.26 \cdot 10^{-1}, 3.14 \cdot 10^{-1}, 0, 0, 0]$	$[3.15 \cdot 10^{-1}, 3.21 \cdot 10^{-1}, 3.16 \cdot 10^{-1}, 0, 0, 0]$
$\boldsymbol{A}^\beta$	$\begin{bmatrix} 3.05 & 1.28 & 1.40 & 0 & 0 & 0 \\ 1.28 & 2.91 & 1.35 & 0 & 0 & 0 \\ 1.40 & 1.35 & 3.02 & 0 & 0 & 0 \\ 0 & 0 & 0 & 0.552 & 0 & 0 \\ 0 & 0 & 0 & 0 & 0.641 & 0 \\ 0 & 0 & 0 & 0 & 0 & 0.611 \end{bmatrix}$	$\begin{bmatrix} 2.99 & 1.08 & 1.30 & 0 & 0 & 0 \\ 1.08 & 2.72 & 1.20 & 0 & 0 & 0 \\ 1.30 & 1.20 & 2.93 & 0 & 0 & 0 \\ 0 & 0 & 0 & 0.519 & 0 & 0 \\ 0 & 0 & 0 & 0 & 0.688 & 0 \\ 0 & 0 & 0 & 0 & 0 & 0.631 \end{bmatrix}$
M^β	$4.66 \cdot 10^{-2}$	$5.68 \cdot 10^{-2}$
$\bar{M}^\beta$	$4.80 \cdot 10^{-2}$	$6.31 \cdot 10^{-2}$
N^β	$-4.73 \cdot 10^{-2}$	$-5.99 \cdot 10^{-2}$

Table 1: Homogenized coefficients on levels α, β for case 1 and 2.

connected porosity (case 2) behaves in a viscoelastic manner because of the fluid flow in the interconnected pores, while the disconnected porosity (case 1) behaves like an elastic body, without time dependence.

4 Conclusion

In this paper we introduced the two-level homogenized model of poroelastic media with weakly permeable interface between two porosities. As an advantage, the poroelastic coefficients can be computed for a given specific micro- and meso- structures. Obviously, this method of introducing the "effective" material parameters is much more accurate than the phenomenological approach based on the theory of porous media, cf. [5, 7]. In the literature, homogenization in poroelasticity is a frequently discussed issue [2], but to our knowledge, the results reported in this paper are novel, namely due to the numerical feedback and computer implementation [3]. There are many issues of interest which should be considered in a future work, such as the restrictions arising along-with the scale separation and periodicity. Moreover, there are several important extensions of the present modeling approach which we have in mind: comparing this hierarchical method of upscaling with the homogenization of double porous media, cf. [17], extensions for nonlinear materials and large deformations [11, 15, 10], or modeling poro-viscoelastic structures, [19, 18].

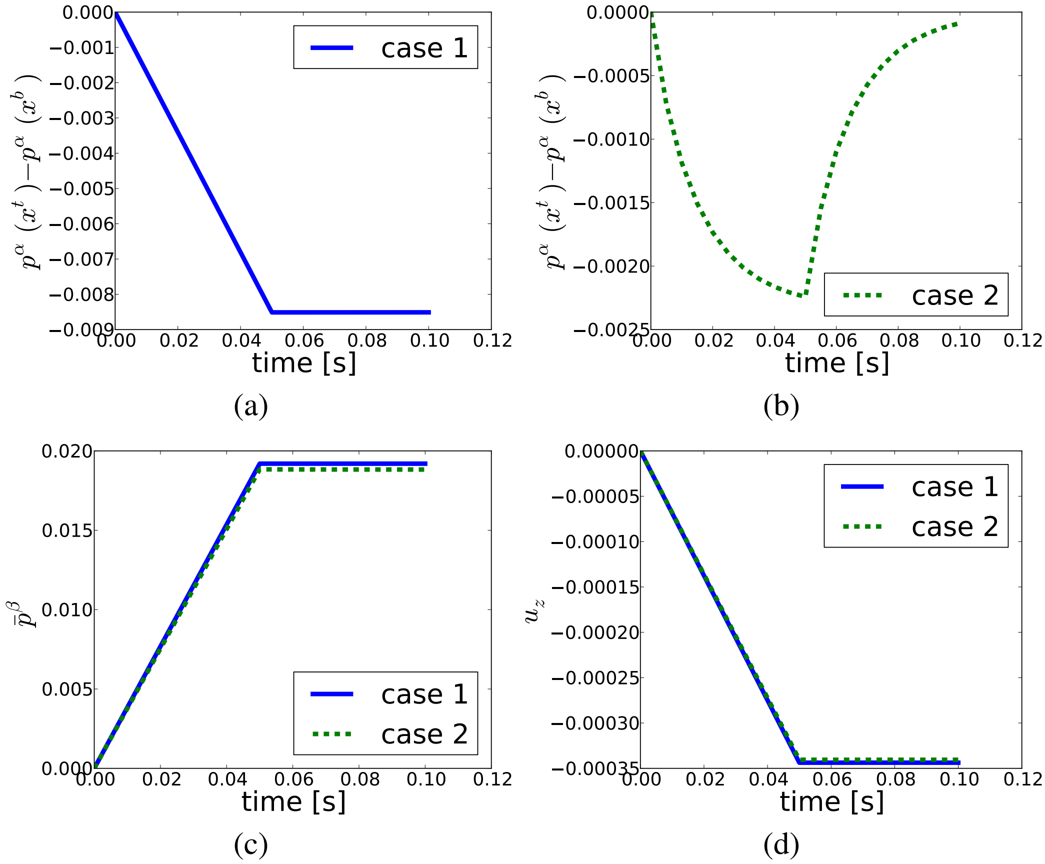

Figure 3: Comparison of time histories of macroscopic solutions for the two cases: (a) difference between p^α in a point on the top face x^t and bottom face x^b for case 1; (b) for case 2; (c) $\bar{p}^\beta$, (d) z-displacement in a point on the top face x^t.

Acknowledgment

The research is supported in part by projects GACR 106/09/0740 of the Czech Republic and by the European Regional Development Fund (ERDF), project "NTIS - New Technologies for Information Society", European Centre of Excellence, CZ.1.05/ 1.1.00/02.0090.

References

[1] T. Arbogast, J. Douglas, U. Hornung, "Derivation of the double porosity model of single phase flow via homogenization theory", *SIAM J. Math. Anal.*, 21: 823–836, 1990.

[2] J.L. Auriault, E. Sanchez-Palencia, "Étude du comportement macroscopique d'un milieu poreux sature deformable", *Jour. de Mécanique*, 16(4): 575–603, 1977.

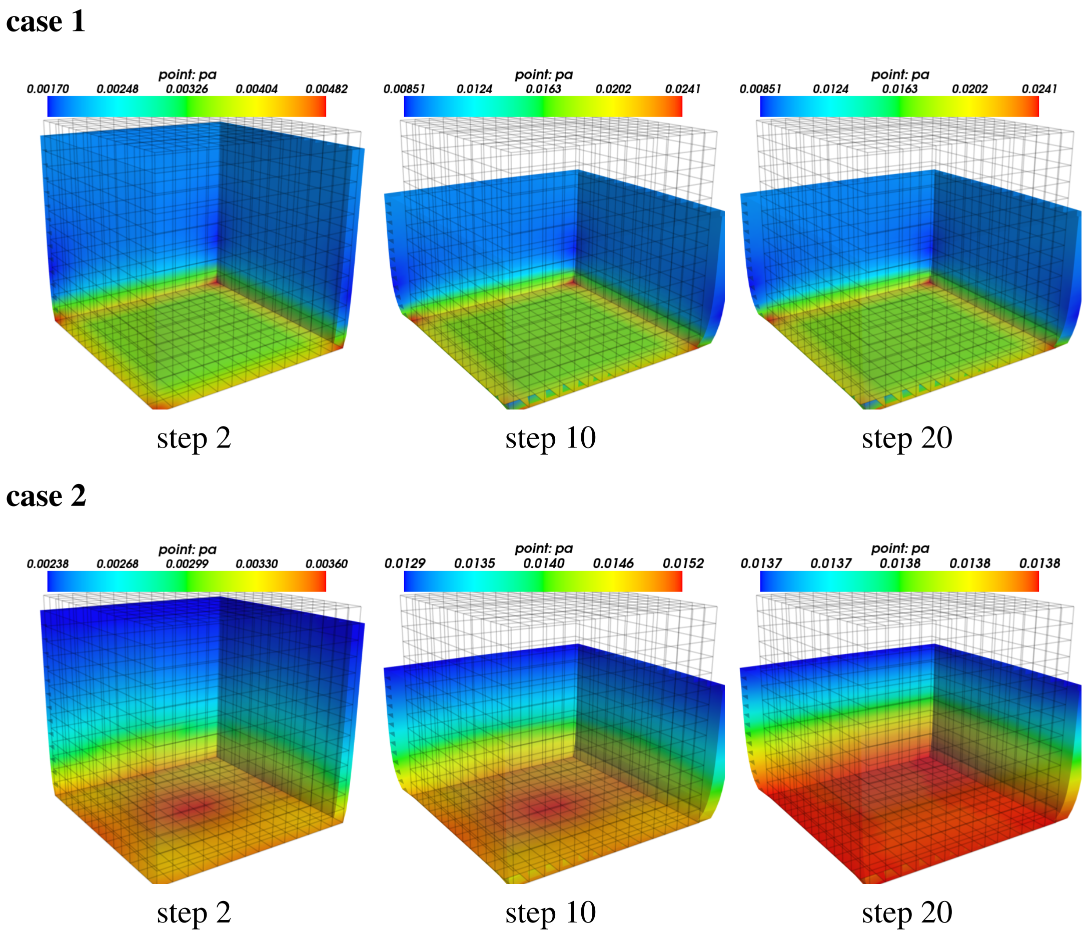

Figure 4: Snapshots of macroscopic solutions ($10\times$ magnified $\boldsymbol{u}$, color = p^α) in time steps 2, 10 and 20 for the case 1 (top) and 2 (bottom). For the case 2, notice the much smaller differencies in p^α over the entirety of Ω, that diminishes to 0 in step 20, as the loading is constant after step 10.

[3] R. Cimrman, contributors, "SfePy: Simple Finite Elements in Python", 2012, URL `http://sfepy.org`, http://sfepy.org.

[4] D. Cioranescu, A. Damlamian, G. Griso, "The periodic unfolding method in homogenization", *SIAM Journal on Mathematical Analysis*, 40(4): 1585–1620, 2008.

[5] O. Coussy, *Poromechanics*, John Wiley & Sons, 2004.

[6] S.C. Cowin, *Bone mechanics handbook*, CRC Press, Boca Raton, FL, 2nd edition, 2001.

[7] L. Dormieux, A. Molinari, D. Kondo, "Micromechanical approach to the behavior of poroelastic materials", *Jour. Mech. Phys. Solids*, 50: 2203–2231, 2002.

[8] G. Griso, E. Rohan, "On the homogenization of a diffusion-deformation problem in strongly heterogeneous media", *Ricerche mat.*, 56: 161–188, 2007.

[9] U. Hornung, *Homogenization and porous media*, Springer, Berlin, 1997.

[10] V. Lukeš, E. Rohan, "Microstructure based two-scale modelling of soft tissues",

Math. and Computers in Simulation, 65(215): 1019–1037, 1996.

[11] E. Rohan, "Modelling large deformation induced microflow in soft biological tissues", *Theor. and Comp. Fluid Dynamics*, 20: 251–276, 2006.

[12] E. Rohan, R. Cimrman, "Two-scale modelling of tissue perfusion problem using homogenization of dual prous media", *Int. Jour. for Multiscale Comput. Engrg.*, 8: 81–102, 2010.

[13] E. Rohan, R. Cimrman, "Multiscale FE simulation of diffusion-deformation processes in homogenized dual-porous media", *Math. Comp. Simul.*, 2011, In Press.

[14] E. Rohan, R. Cimrman, V. Lukeš, "Numerical modelling and homogenized constitutive law of large deforming fluid saturated heterogeneous solids", *Computers and Structures*, 84: 1095–1114, 2006.

[15] E. Rohan, V. Lukeš, "Homogenization of perfusion in large-deforming medium using the Updated Lagrangian Formulation", in *Proceedings of the ECT 2010 conference*. Coburg-Sax Publ., 2010.

[16] E. Rohan, S. Naili, R. Cimrman, T. Lemaire, "Hierarchical homogenization of fluid saturated porous solid with multiple porosity scales", *Compte Rendus Acad. Sci./Mécanique*, 2012, Submitted.

[17] E. Rohan, S. Naili, R. Cimrman, T. Lemaire, "Multiscale modelling of a fluid saturated medium with double porosity: relevance to the compact bone", *Jour. Mech. Phys. Solids*, 60: 857881, 2012.

[18] E. Rohan, S. Shaw, M.F. Wheeler, J.R. Whiteman, "Mixed and Galerkin finite element approximation of flow in a linear viscoelastic porous medium", Technical report, BICOM, Brunel University, 2012, Technical Report 12/2, `www.brunel.ac.uk/bicom`.

[19] E. Rohan, S. Shaw, J.R. Whiteman, "Poro-viscoelasticity modelling based on upscaling quasistatic fluid-saturated solids", Technical report, BICOM, Brunel University, 2012, Technical Report 12/1, `www.brunel.ac.uk/bicom`.

[20] E. Sanchez-Palencia, *Non-homogeneous media and vibration theory*, Number 127 in Lecture Notes in Physics. Springer, Berlin, 1980.